Critical phenomena of a hybrid phase transition in cluster merging dynamics

K. Choi,[1] Deokjae Lee,[1] Y. S. Cho,[2] J. C. Thiele,[3] H. J. Herrmann,[3] and B. Kahng[1,*]

[1]*CCSS, CTP, and Department of Physics and Astronomy, Seoul National University, Seoul 08826, Korea*

[2]*Department of Physics, Chonbuk National University, Jeonju 54896, Korea*

[3]*Computational Physics for Engineering Materials, Institute for Building Materials, ETH Zürich, 8093 Zürich, Switzerland*

(Received 19 June 2017; revised manuscript received 21 August 2017; published 24 October 2017)

Recently, a hybrid percolation transition (HPT) that exhibits both a discontinuous transition and critical behavior at the same transition point has been observed in diverse complex systems. While the HPT induced by avalanche dynamics has been studied extensively, the HPT induced by cluster merging dynamics (HPT-CMD) has received little attention. Here, we aim to develop a theoretical framework for the HPT-CMD. We find that two correlation-length exponents are necessary for characterizing the giant cluster and finite clusters separately. The conventional formula of the fractal dimension in terms of the critical exponents is not valid. Neither the giant nor finite clusters are fractals, but they have fractal boundaries. A finite-size scaling method for the HPT-CMD is also introduced.

DOI: 10.1103/PhysRevE.96.042148

I. INTRODUCTION

Percolation has long served as a simple model that undergoes a geometrical phase transition in nonequilibrium disordered systems [1]. As an occupation probability p is increased beyond a transition point p_c, a macroscopic-scale giant cluster emerges across the system. This percolation theory has been used for understanding percolation-related diverse phenomena such as conductor-insulator transitions [2], the resilience of systems [3–5], the formation of public opinion [6,7], and the spread of disease in a population [8,9]. The theory of percolation transition was well established by the Kasteleyn-Fortuin formula [10]. The percolation transition is known to be one of the most robust continuous transitions [1,11].

Recently, however, many explosive or abrupt percolation transitions have been observed in complex systems [12–18], such as large-scale blackouts in power-grid systems [19] and pandemics [20], in which the order parameter increases or decreases abruptly at a transition point. In such phenomena, when a system is perturbed, e.g., when a link is removed, an avalanche dynamics occurs, which leads the order parameter to collapse to zero at a transition point. The transitions in k-core percolation [21–25] and in the cascading failure model on interdependent networks [19,26–29] are prototypical instances. In these models, hybrid percolation transitions (HPTs) can be induced by avalanche dynamics. The order parameter exhibits a second-order and a first-order transition at the same transition point. However, the cluster-size distribution (CSD) does not follow a power law, thus the conventional percolation theory could not be applied to this type of HPT. Instead, the theory of critical avalanche dynamics was applied to understand the critical behavior of the HPT [24,27,29].

At this stage, one may be interested in a HPT generated as links are added one by one, similarly to the kinetics of ordinary percolation and explosive percolation [12]. Thus, the HPT is induced by cluster merging dynamics (abbreviated as HPT-CMD). Actually, we introduced a modified version [30] of the so-called half-restricted percolation model [31] for this purpose, and we obtained interesting mean-field results [30]. As links are added to a system, the order parameter (i.e., the fraction of nodes belonging to a giant cluster) remains zero up to a transition point, at which it increases rapidly to a finite value, generating a first-order transition. During this increase process, clusters are self-organized in their sizes, after which the size distribution of finite clusters follows a power law. A giant cluster is located separately from those finite clusters in the CSD. As more links are added to the system, the order parameter increases gradually, and a second-order transition occurs. Indeed, the properties of the second-order transition are determined by the power-law behavior of the CSD. In this paper, we aim to develop a theoretical framework for a HPT-CMD using the restricted percolation model in two dimensions and the mean-field result. We find that two correlation-length exponents ν_g and ν_s are needed to characterize the critical behaviors of the giant cluster and finite clusters, respectively. To explore HPTs, we introduce a finite-size scaling method that is more advanced than the method used in the second-order percolation transition.

This paper is organized as follows: In Sec. II, we recall the theory of ordinary percolation for further discussion in the HPT. In Sec. III, we introduce the restricted percolation model and explain the underlying mechanism of the dynamic rule and why this model generates a HPT-CMD. The conventional finite-size scaling method cannot be applied to a hybrid percolation transition. In Sec. IV, we present a finite-size scaling method that is applicable to the hybrid percolation transition. In Sec. V, we use this method to determine the values of critical exponents for the restricted percolation model. In Sec. VI, we determine the fractal dimensions of finite clusters and the giant cluster, and we show that the conventional formula for the fractal dimension in terms of the critical exponents is not satisfied. The final section is devoted to a discussion and a summary.

II. PERCOLATION THEORY

We first recall the theory of continuous percolation transitions [1]. The order parameter increases from zero continuously as $m \sim (p - p_c)^{\beta}$ for $p > p_c$; the mean cluster

*bkahng@snu.ac.kr

size diverges as $\langle s\rangle \sim |p-p_c|^{-\gamma}$, and the correlation length diverges as $\xi \sim |p-p_c|^{-\nu}$. These exponents satisfy the hyperscaling relation $2\beta+\gamma = d\nu$, where d is the spatial dimension. The critical exponents and the scaling relations can be obtained from the CSD denoted as $n_s(p)$, which behaves as $n_s(p) \sim s^{-\tau}\exp(-s/s^*)$, where $s^* \sim (p-p_c)^{-1/\sigma}$. On the other hand, a percolating cluster at p_c is a fractal object. The total number of sites belonging to this percolating cluster, denoted as $M_\infty(L)$, where L is the linear size of the system in Euclidean space, scales as $M_\infty(L) \sim L^D$, where D is the fractal dimension. In addition to the percolating cluster, finite clusters also behave similarly, as $M_s(R_s) \sim R_s^D$, where R_s is the linear size of an s-size cluster. The fractal dimension D is related to the critical exponents β and ν as $D = d - \beta/\nu$.

III. THE r-PERCOLATION MODEL IN TWO DIMENSIONS

We begin with the introduction of the so-called restricted percolation model on a square lattice of size $L \times L$. $N = L^2$ is the total number of sites in the system. Bonds are occupied on the lattice one by one at each time step according to a given rule [32]. When b bonds are occupied in the system, the occupation probability p conventionally used in bond percolation corresponds to $p = b/(2N)$. Here we use a control parameter $t = b/N$, which is the same as $t = 2p$. The dynamic rule of bond occupation is as follows: At each time step, we classify clusters into two sets, a set R and its complement set R^c according to their sizes. Let c_i denote the ith cluster in ascending size order. The set R contains the k smallest clusters, those satisfying $\sum_{i=1}^{k-1} s(c_i) < \lfloor gN \rfloor \leqslant \sum_{i=1}^{k} s(c_i)$, where $s(c_i)$ denotes the size of the cluster with index c_i, and $g \in (0,1]$ is a parameter that controls the size of the set R. The complement of R, denoted as R^c, contains the remaining largest clusters. Next, we occupy a randomly chosen unoccupied bond, one or both ends of which belong to the clusters in the set R. We do not allow the occupation of bonds between two sites belonging to clusters in the set R^c. We remark that our dynamic rule is slightly different from the original one in the following point: when $\lfloor gN \rfloor < \sum_{i=1}^{k} s(c_i)$, in the original model, some $\lfloor gN \rfloor - \sum_{i=1}^{k-1} s(c_i)$ nodes in the kth cluster belong to the set R, and the remaining nodes in the kth cluster belong to the set R^c, whereas in our model all nodes in the kth cluster belong to the set R. We call this model the restricted percolation (abbreviated as r-percolation) model with reference to the original name, i.e., the half-restricted percolation model [31]. We use periodic boundary conditions in the simulations.

This r-percolation model contains two important factors to generate a HPT-CMD. The first is to attain global information, which is needed to generate a discontinuous percolation transition as proposed in Ref. [13]. At each dynamic step, we need to order all clusters according to their sizes. This ordering cannot be achieved without global information about all cluster sizes. The other is to create a continuous transition. As the size of a giant cluster exceeds $(1-g)N$, the giant cluster lies on the boundary of the sets R and R^c. Then according to the modified rule, it belongs to the set R and thus the model is no longer restrictive, but it reduces to ordinary percolation. Thus, a second-order transition naturally occurs. Our modified rule is much simpler in simulations, and it also enables us to solve the critical behavior analytically for the mean-field case [30]. Accordingly, as $g \to 1$, $m_0 \to 0$, and our model reduces to the ordinary percolation model and undergoes a second-order transition.

For explosive percolation, when the number of link candidates is larger than two, denoted as k_e, the critical exponent β depends on k_e [33–35]. Thus, the exponent is continuously varying. Note that k_e serves as a parameter that controls the extent of attaining global information. Moreover, as k_e increases, the growth of the giant cluster becomes more suppressed. In the r-percolation model, the parameter $(1-g)$ plays a similar role. Thus, the critical exponents depend on g (see Table I and Fig. 8). These features may be reminiscent of the previous work in which the n-component spin model with long-range interactions $1/r^{d+\eta}$ $(0 < \eta < 2)$ exhibits a continuous transition with η-dependent critical exponents [36].

IV. FINITE-SIZE SCALING METHOD

Determining a transition point t_c is not straightforward in the HPT-CMD. We first obtain the distribution $P(m;t,L)$ of the order parameter m by accumulating different configurations with m for fixed t and L. Next, we characterize two time steps, $t_c^-(L)$ and $t_c^+(L)$. For $t \leqslant t_c^-(L)$, $P(m;t,L)$ exhibits a peak at a certain m near $m = 0$ denoted as $m^-(L)$. $m^-(L)$ is denoted as $m_*^-(L)$ at a particular point $t = t_c^-(L)$, which satisfies the criterion that for $t > t_c^-(L)$, $P(m)$ begins to exhibit another peak at $m^+(L)$ near $m = 1$, as shown in Fig. 1. As t is increased further, the peak at m^- shrinks, whereas the other peak at m^+ becomes higher. At $t = t_c^+(L)$, the peak at m^- disappears, and only the peak at m_*^+ remains. For $t > t_c^+(L)$, a peak remains at $m^+(L)$, which grows with t. As L is increased, $t_c^-(L)$ and $t_c^+(L)$ converge to a certain value t_c, and $m^-(L) \to 0$, and $m^+(L)$ approaches a certain value m_0.

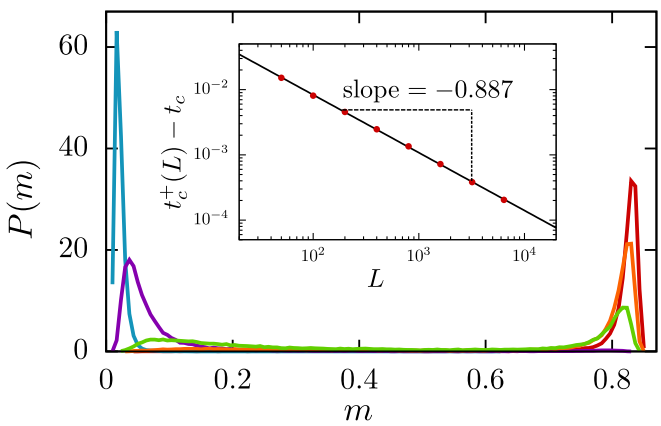

FIG. 1. Plot of the distributions of the order parameter for $L = 6400$. The distribution is unimodal with a peak near zero (left peak) for $t < t_c^-(L)$ (light blue and violet). As t passes $t_c^-(L)$ (light green), the right peak begins to grow, whereas the left-hand peak shrinks. As t reaches $t_c^+(L)$ (orange), the left peak disappears and the distribution becomes unimodal with the right peak alone. The two characteristic times $t_c^-(L)$ and $t_c^+(L)$ converge to a transition point t_c in the thermodynamic limit. The inset shows the scaling behavior $t_c^+(L) - t_c \sim L^{-1/\nu_g'}$.

This suggests that the order parameter exhibits a discontinuous jump at t_c in the thermodynamic limit. Particularly, we find that $t_c^+(L) - t_c \sim L^{-1/\nu_g'}$, in which the exponent ν_g' is estimated to be $\nu_g' \approx 1.13 \pm 0.07$ for $g = 0.5$ (see the inset of Fig. 1).

The majority of realizations have no giant cluster in $t < t_c^-(L)$ and have a giant cluster in $t > t_c^+(L)$ in contrast to the situation in $t_c^-(L) < t < t_c^+(L)$. Thus the ensemble average taken over the realizations in those separate regions can be easily calculated. Moreover, the finite-size effect is still observed near $t_c^-(L)$ and $t_c^+(L)$. Thus we use the simulation data obtained only in $t < t_c^-(L)$ or $t > t_c^+(L)$ for finite-size-scaling analysis and discard the data obtained in $t_c^-(L) < t < t_c^+(L)$. The asymptotic behavior of the system at $t_c^+(L)$ as $L \to \infty$ gives the behavior of the system as t approaches t_c from above in the thermodynamic limit, i.e., the properties of the percolating phase near the critical point. Similarly, the properties of the nonpercolating phase near the critical point are obtained by observing the system at $t_c^-(L)$. For instance, the scaling plot of $(m - m_0)L^{\beta/\nu_g}$ versus $(t - t_c)L^{1/\nu_g}$ can be drawn in the region $t \geqslant t_c^+(L)$, which will be shown later. This numerical analysis method differs from those in the ordinary percolation transitions. For the simulations of continuous percolation transitions, we do not need to investigate the two limits separately, and we also do not need to distinguish the two phases strictly around the transition point.

V. CRITICAL EXPONENT VALUES AND HYPERSCALING RELATIONS

In finite systems, the order parameter $m(t)$ is approximately $m^-(L)$ for $t \leqslant t_c^-(L)$, but it increases rapidly in the interval $t_c^-(L) < t < t_c^+(L)$, and it becomes $m_*^+(L)$ at $t_c^+(L)$, beyond which it increases gradually as t is increased, as shown in Fig. 2. This suggests that in the thermodynamic limit, $m(t)$ behaves as

$$m(t) = \begin{cases} 0 & \text{for } t < t_c, \\ m_0 + r(t - t_c)^\beta & \text{for } t \geqslant t_c, \end{cases} \tag{1}$$

where m_0 and r are constants. m_0 represents the fraction of sites belonging to the giant cluster at t_c, and the second term

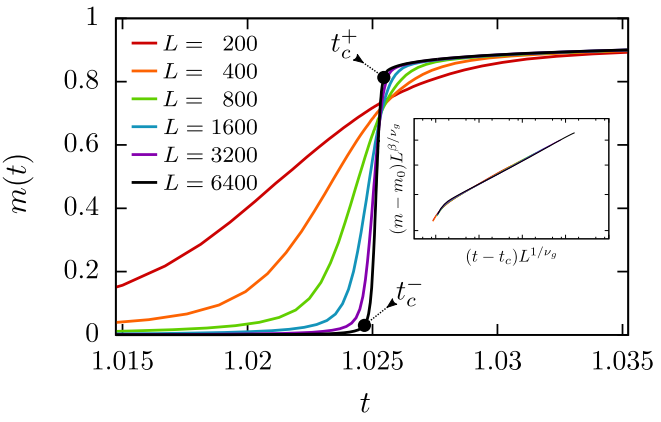

FIG. 2. Plot of the order parameter $m(t)$ vs t for the restricted percolation model with $g = 0.5$ for different lateral sizes L and in data collapse form of $(m - m_0)L^{\beta/\nu_g}$ vs $(t - t_c)L^{1/\nu_g}$ (inset). Characteristic time steps t_c^- and t_c^+ for $L = 6400$ are marked.

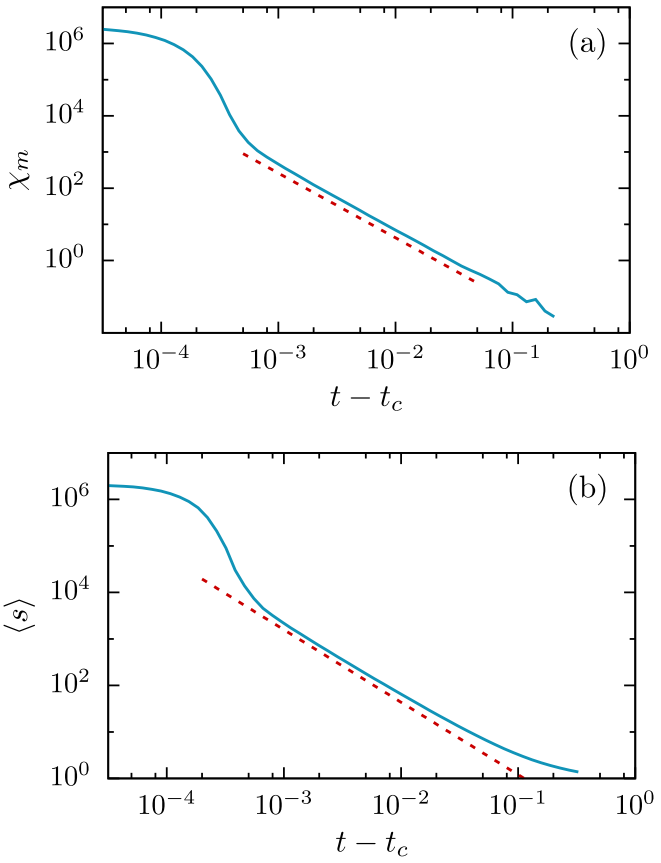

FIG. 3. (a) Plot of the susceptibility defined as $\chi_m = L^2(\langle m^2 \rangle - \langle m \rangle^2)$ vs $t - t_c$. $\chi_m \sim (t - t_c)^{-\gamma_m}$ is expected. The dashed line is a guideline with slope -1.79. The susceptibility exponent is obtained as $\gamma_m = 1.79 \pm 0.08$. (b) Plot of the susceptibility defined as $\chi_s = \langle s \rangle \sim \sum_{s=1}^{\text{finite}} s^2 n_s$ vs $t - t_c$. $\chi_s \sim (t - t_c)^{-\gamma_s}$ is expected. The dashed line is a guideline with slope -1.56. The susceptibility exponent is obtained as $\gamma_s = 1.56 \pm 0.15$. Simulation data are obtained from the systems with lateral size $L = 6400$.

represents the increment of the order parameter as t is increased beyond t_c. In finite systems, the order parameter for $t > t_c$ may be written as $m(t) - m_0 \sim L^{-\beta/\nu_g}$ in the critical region above t_c, in which L is less than the correlation length of the giant cluster, $\xi_g \sim (t - t_c)^{-\nu_g}$. β is determined as $\beta = 0.061 \pm 0.005$ for $g = 0.5$ by plotting $m - m_0$ versus $t - t_c$, while ν_g is determined as $\nu_g = 1.03 \pm 0.08$ by plotting $(m - m_0)L^{\beta/\nu_g}$ versus $(t - t_c)L^{1/\nu_g}$ (see Fig. 2). Because the numerical values of ν_g and ν_g' agree within the error bars, we may regard them as being the same. We examine the susceptibility in the form of the fluctuations of the order parameter. We obtain the associated exponent as $\gamma_m = 1.79 \pm 0.08$ for $g = 0.5$ in Fig. 3. The scaling relation $2\beta + \gamma_m = d\nu_g$ is satisfied within error bars.

The CSD $n_s(t)$ of finite clusters exhibits a power-law decay with the exponent τ at a transition point t_c. This is an important feature of the critical behavior of the HPT-CMD. In finite systems, the power-law behavior occurs at $t_c^+(L)$ (see Fig. 4), which is reduced to t_c as $L \to \infty$. When $t > t_c$, the CSD of finite clusters exhibits a crossover behavior at s^*: $n_s(t) \sim s^{-\tau} e^{-s/s^*}$, where $s^* \sim (t - t_c)^{-1/\sigma}$. We obtain the exponents τ and σ from Fig. 4. Using the results of $\tau = 2.035 \pm 0.009$ and $\sigma = 0.58 \pm 0.03$ for $g = 0.5$ and

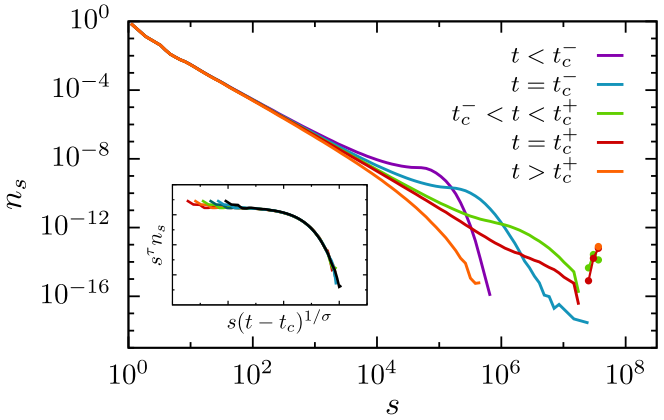

FIG. 4. Plot of the size distribution of finite clusters $n_s(t)$ and the giant cluster (separated dots) at various time steps for $L = 6400$ and $g = 0.5$. At $t < t_c^+(L)$, a bump exists in the tail part, but it shrinks as t increases, and it finally disappears at $t = t_c^+(L)$. Inset: scaling plot of the size distribution of finite clusters in the form of $s^\tau n_s$ vs $s(t - t_c)^{1/\sigma}$ for several $t > t_c$.

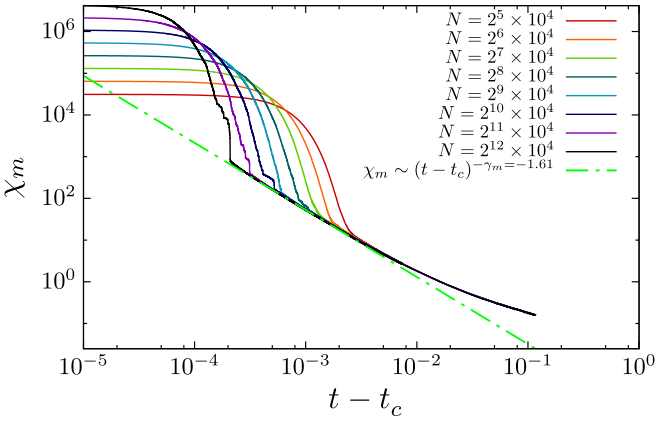

FIG. 6. Plot of the susceptibility defined as $\chi_m = L^2[\langle m^2 \rangle - \langle m \rangle^2]$ vs $t - t_c$. $\chi_m \sim (t - t_c)^{-\gamma_m}$ is expected. The dashed-dotted line is a guideline with slope -1.61. The susceptibility exponent is obtained as $\gamma_m = 1.61 \pm 0.12$, which satisfies the scaling relation $2\beta + \gamma_m = \bar{\nu}_g$. The system sizes are chosen as $N = 2^5 \times 10^4$ and $2^{12} \times 10^4$.

the scaling relation $\beta = (\tau - 2)/\sigma$, we determine the critical exponent β as 0.0613 ± 0.0187 for $g = 0.5$. This value is consistent with the directly measured one within error bars. We examine the susceptibility in the form of the second moment of the size distribution of finite clusters, and we obtain the associated exponent as $\gamma_s = 1.56 \pm 0.15$. The scaling relation $\gamma_s = (3 - \tau)/\sigma$ is satisfied within error bars.

Introducing the correlation length exponent ν_s of finite clusters, we obtain that $s^* \sim L^{1/\sigma\nu_s}$. We numerically obtain that $1/(\sigma\nu_s) \approx 1.9523 \pm 0.0045$ for $g = 0.5$ by measuring the ratio of the $(n + 1)$th moment of $n_s(t)$ to the nth moment, where $n \geqslant 3$. Using the previously obtained value $\sigma = 0.58 \pm 0.03$ for $g = 0.5$, we obtain $\nu_s = 0.886 \pm 0.048$. Using the directly measured values $\tau = 2.035 \pm 0009$ and $d = 2$, we find that the hyperscaling relation $d\nu_s = (\tau - 1)/\sigma$ holds. The values of those critical exponents depend on the parameter g. Their values are listed in Table I and shown in Fig. 8.

In previous studies [30], we found numerically that $\beta = 0.21 \pm 0.05$, $\gamma_s = 0.83 \pm 0.05$, $1/\sigma = 1.04 \pm 0.05$, and $\tau =$ 2.18 ± 0.04 for $g = 0.5$ for the r-percolation model in Erdös-Rényi (ER) networks. These exponent values yield the value of correlation size as $\bar{\nu}_s \equiv d\nu_s = (\tau - 1)/\sigma \approx 1.23 \pm 0.10$ for finite clusters. Here we obtain the exponent value of the correlation length exponent for $g = 0.5$ as $\bar{\nu}_g \equiv d\nu_g \approx 2.0$ for the giant cluster using the data collapse technique for the formula $[m(t) - m_0]N^{\beta/\bar{\nu}_g}$ versus $(t - t_c)N^{1/\bar{\nu}_g}$ for different system sizes (Fig. 5). Therefore, the two exponents, $\bar{\nu}_g$ and $\bar{\nu}_s$, are different even in the mean-field version of the r-percolation

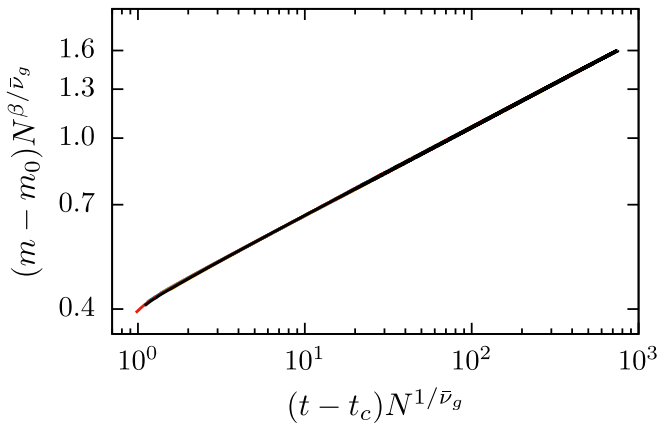

FIG. 5. Plot of the order parameter $m(t)$ vs t for the r-ER percolation model with $g = 0.5$ for different system sizes N in data collapse form of $(m - m_0)N^{\beta/\bar{\nu}_g}$ vs $(t - t_c)N^{1/\bar{\nu}_g}$. $\bar{\nu}_g$ is estimated to be ≈2.0. The system sizes are chosen as $N = 10^4$ and $2^{12} \times 10^4$.

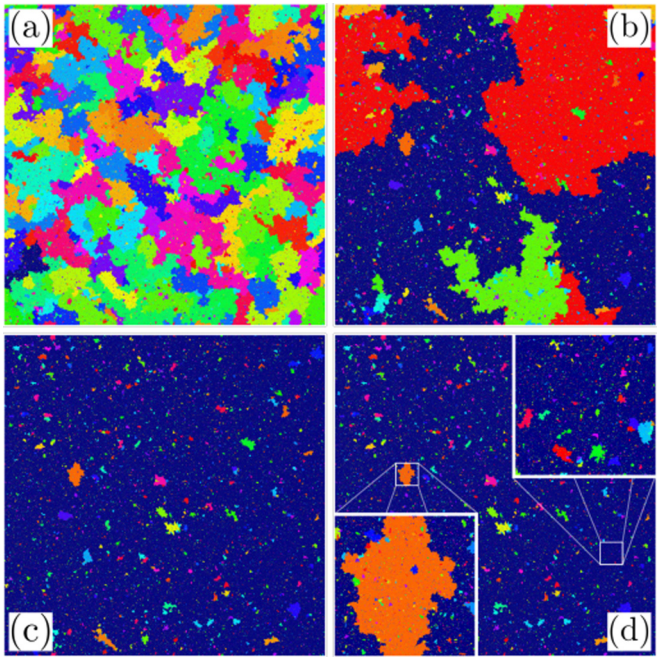

FIG. 7. Snapshots of the system of lateral size $L = 6400$ with $g = 0.5$ at three time steps (a) $t = t_c^- \approx 1.024\,573\,46$, (b) $t_c \approx 1.025\,23$, and (c) $t_c^+ \approx 1.025\,434\,37$. At t_c^+, the size distribution of finite clusters follows a power law. (d) Zoom-in snapshots of the giant cluster (top right) and a finite cluster (lower left).

TABLE I. The critical exponents for the r-percolation model with general g in two dimensions.

g	t_c	m_0	β	γ_m	τ	σ	γ_s	ν_g'	ν_g	ν_s
0.1	1.06381 ± 0.00004	0.98 ± 0.05	0.003 ± 0.005	2.07 ± 0.25	1.918 ± 0.035	0.61 ± 0.04	1.77 ± 0.25	1.06 ± 0.07	0.95 ± 0.12	0.848 ± 0.069
0.2	1.06019 ± 0.00004	0.88 ± 0.05	0.016 ± 0.008	1.69 ± 0.15	1.993 ± 0.015	0.60 ± 0.03	1.56 ± 0.15	1.07 ± 0.07	0.95 ± 0.10	0.848 ± 0.046
0.3	1.05124 ± 0.00004	0.80 ± 0.05	0.038 ± 0.008	1.68 ± 0.08	2.023 ± 0.015	0.60 ± 0.03	1.53 ± 0.15	1.07 ± 0.07	0.99 ± 0.10	0.840 ± 0.048
0.4	1.03903 ± 0.00005	0.68 ± 0.05	0.051 ± 0.005	1.73 ± 0.08	2.030 ± 0.010	0.58 ± 0.03	1.55 ± 0.15	1.09 ± 0.05	1.02 ± 0.08	0.883 ± 0.050
0.5	1.02523 ± 0.00005	0.55 ± 0.03	0.061 ± 0.005	1.79 ± 0.08	2.035 ± 0.009	0.58 ± 0.03	1.56 ± 0.15	1.13 ± 0.07	1.03 ± 0.08	0.886 ± 0.048
0.6	1.01151 ± 0.00005	0.49 ± 0.05	0.086 ± 0.005	1.89 ± 0.08	2.047 ± 0.009	0.55 ± 0.03	1.64 ± 0.15	1.14 ± 0.07	1.09 ± 0.08	0.929 ± 0.052
0.7	0.99855 ± 0.00006	0.36 ± 0.05	0.098 ± 0.005	2.01 ± 0.08	2.050 ± 0.009	0.51 ± 0.03	1.77 ± 0.15	1.14 ± 0.07	1.11 ± 0.09	1.009 ± 0.061
0.8	0.98775 ± 0.00006	0.23 ± 0.05	0.108 ± 0.005	2.08 ± 0.08	2.052 ± 0.008	0.49 ± 0.03	1.79 ± 0.15	1.13 ± 0.07	1.15 ± 0.08	1.062 ± 0.066
0.9	0.98167 ± 0.00010	0.10 ± 0.05	0.120 ± 0.008	2.24 ± 0.08	2.053 ± 0.009	0.44 ± 0.03	2.03 ± 0.17	1.11 ± 0.11	1.20 ± 0.09	1.196 ± 0.083
1.0	1	0	5/36(0.139)		187/91(2.055)	36/91(0.40)	43/18(2.39)		4/3(1.33)	

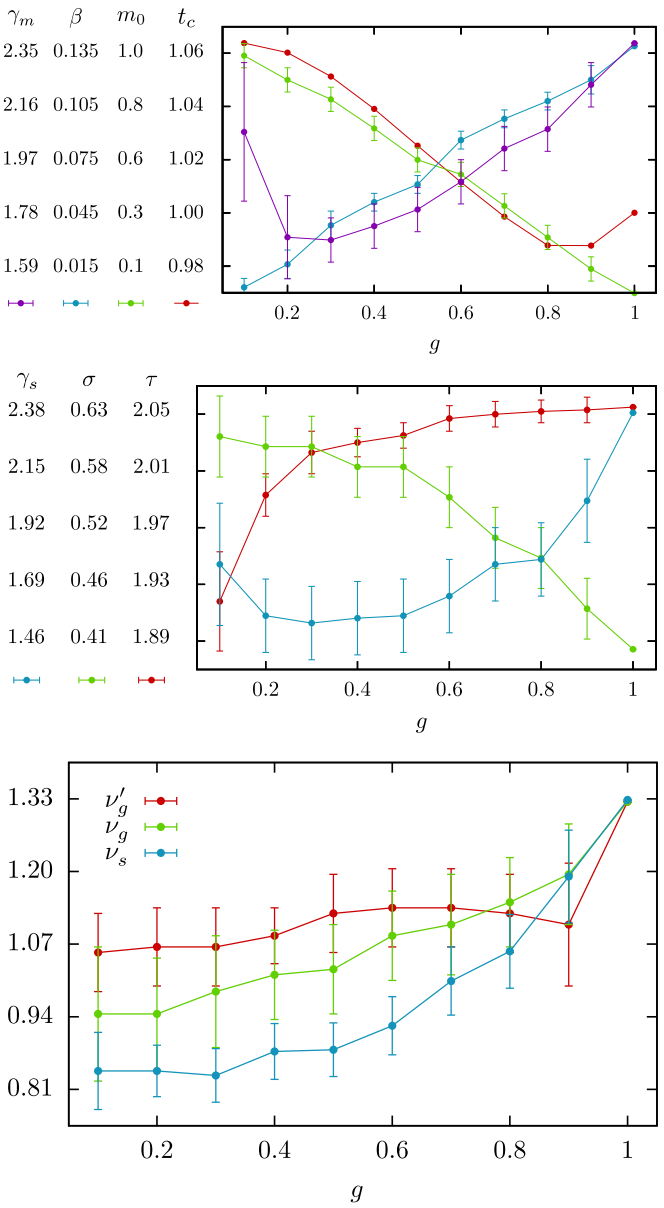

FIG. 8. The critical exponents for the r-percolation model with general g in two dimensions. This is a graphical representation of Table I. Data for $g = 0.1$ could be distorted by huge error bars caused by the crossover behavior to a discontinuous transition as $g \to 0$.

model. We also measure the susceptibility exponent γ_m for the giant cluster for $g = 0.5$ as $\gamma_m \approx 1.61 \pm 0.12$ (Fig. 6). Thus, we find that the hyperscaling relation $2\beta + \gamma_m = \bar{\nu}_g$ is satisfied.

VI. FRACTAL DIMENSIONS

Next, we are interested in the fractal dimensions of the giant and finite clusters. Here we determine these fractal dimensions using the box-covering method as follows: For a given cluster, we determine its center of mass. Then we open a window of size $\ell \times \ell$, the center of which is placed at the center of mass of the cluster. We count the number of occupied sites within the window, which is called the mass, $M(\ell)$. We obtain

the average mass of the giant cluster, $M_\infty(\ell)$, over different configurations, and the average mass of finite clusters of size s, $M_s(\ell)$, over different clusters of the same size s and different configurations. We also calculate the mean radius of gyration of all clusters of size s, denoted as R_s.

We measure the fractal dimension D_g of the giant cluster using the relation $M_\infty(\ell) \sim \ell^{D_g}$ for each system size L at a transition point $t_c^+(L)$. As shown in Fig. 7, the clusters are almost compact, and we obtain that $D_g = 2.0001 \pm 0.003$ regardless of L. We measure the fractal dimension of finite clusters using the relation $M_s(\ell)/s \sim (\ell/R_s)^{D_s}$. We obtain that $D_s = 1.993 \pm 0.010$ independent of the system size L. Therefore, we conclude that neither the giant cluster nor finite clusters are fractal in hybrid percolation. The conventional formalisms of the fractal dimension, $D = d - \beta/\nu$ and $D = 1/\sigma\nu$, are not valid for the HPT-CMD. We remark that the transition point $t_c^+(L)$ of the HPT-CMD is larger than that of the ordinary bond percolation model, $t_c = 1$. Thus, the number of occupied bonds in the critical region of the HPT-CMD is as dense as that in the supercritical region of ordinary percolation. Accordingly, the giant cluster as well as the finite clusters are almost compact with dimension $D_g = D_s = 2$. On the other hand, we examine the fractal property of the perimeter of the largest cluster at t_c. Using the yardstick method, we find that the accessible boundaries of the compact clusters at t_c are fractal with a dimension less than $4/3$ for $g < 1$. We speculate that the fractal dimension of the boundary is the same as $D_b \approx 1.217 \pm 0.001$, the fractal dimensions of the watershed [37], and the Gaussian model for the explosive percolation [38].

VII. DISCUSSION AND SUMMARY

Thus far, we obtained that for the HPT-CMD, there exist two correlation exponents ν_g and ν_s, the percolating cluster and finite clusters are compact, and the fractal dimension reduces to $D_g = D_s = 2 = d$. The properties of the cluster-size distribution in the ordinary percolation can be obtained by using the Kasteleyn-Fortuin formalism for the q-state Potts model in the limit $q \to 1$. On the other hand, in such equilibrium spin models, the critical behavior can be understood using the renormalization-group (RG) transformation of the singular part of the free-energy function f. That is, $f(t,h) = \ell^{-d} f(t',h')$, where t and h are reduced temperature and external field, respectively, and $t' = \ell^{y_t} t$ and $h' = \ell^{y_h} h$, where $y_t = 1/\nu$, $y_h = D$, and ℓ is the scale factor of coarse-grained length. On the other hand, for a discontinuous transition, $y_t = y_h = d$, because of $\beta = 0$ [39]. For the HPT-CMD, we found that there exist two ν exponents ν_g and ν_s, and $D = d$. Thus, it is not clear how to coarse-grain clusters near the transition point. Thus, further studies are needed in the perspective of RG theory.

One may wonder how the HPT-CMD is related to the HPT induced by avalanche dynamics. For the former, the order parameter increases continuously at a transition point in finite systems, but it becomes discontinuous in the thermodynamic limit. For the latter, it jumps or drops suddenly through an avalanche dynamics even in finite systems. The order parameter behaves as in a spinodal transition. Recent studies [25,29] on the HPT by avalanche dynamics such as k-core percolation transitions on Erdös and Rényi networks and the percolation transition on interdependent networks revealed that two sets of critical exponents are needed to characterize the HPT. One is for the order parameter and the other is for the avalanche size distribution, which plays the role of the CSD for the HPT-CMD. One more noteworthy result is that the HPT induced by avalanche dynamics has an intrinsic scaling relation between the critical exponent γ_a of mean avalanche size and the exponent β as $\gamma_a = 1 - \beta$ [29]. However, the analogous relation $\gamma_s = 1 - \beta$ does not hold in the HPT-CMD, because $\sigma_s \neq 1$ for any g. Furthermore, k-core percolation does not occur in two dimensions. Thus, it is not clear how these two cases are related to each other.

In summary, we investigated the critical phenomena of an HPT-CMD using the r-percolation model. We showed that two sets of the critical exponents, including the correlation length exponent, are necessary to understand the critical behaviors for the giant cluster and finite clusters separately. We found that the conventional relationship $D = d - \beta/\nu$ breaks down. Because ν and D play a central role in the RG transformation, our results reveal a fundamental problem, namely how to understand the HPT-CMD in the RG framework. We introduced a finite-sized scaling method to determine the critical exponents in finite systems for the HPT-CMD.

ACKNOWLEDGMENTS

This work was supported by the National Research Foundation of Korea by Grant No. NRF-2014R1A3A2069005. H.J.H. thanks the European Research Council (ERC) for financial support under Advanced Grant No. 319968-FlowCCS.

K.C. and D.L. contributed equally to this work.

[1] D. Stauffer and A. Aharony, *Introduction to Percolation Theory*, 2nd ed. (Taylor and Francis, London, 1994).
[2] D. S. McLachlan, M. Blaszkiewicz, and R. E. Newnham, J. Am. Ceram. Soc. **73**, 2187 (1990).
[3] R. Albert, H. Jeong, and A. L. Barabási, Nature (London) **406**, 378 (2000).
[4] R. Cohen, K. Erez, D. ben-Avraham, and S. Havlin, Phys. Rev. Lett. **85**, 4626 (2000).
[5] F. Morone and H. A. Makse, Nature (London) **524**, 65 (2015).
[6] D. J. Watts, Proc. Natl. Acad. Sci. USA **99**, 5766 (2002).
[7] J. Shao, S. Havlin, and H. E. Stanley, Phys. Rev. Lett. **103**, 018701 (2009).
[8] J. D. Murray, *Mathematical Biology*, 3rd ed. (Springer, Berlin, 2005).
[9] R. Pastor-Satorras, C. Castellano, P. van Mieghem, and A. Vespignani, Rev. Mod. Phys. **87**, 925 (2015).
[10] P. W. Kasteleyn and C. M. Fortuin, J. Phys. Soc. Jpn. Suppl. **26**, 11 (1969).
[11] N. Araújo, P. Grassberger, B. Kahng, K. J. Schrenk, and R. M. Ziff, Eur. Phys. J.: Spec. Top. **223**, 2307 (2014).

[12] D. Achlioptas, R. M. D'Souza, and J. Spencer, Science **323**, 1453 (2009).
[13] O. Riordan and L. Warnke, Science **333**, 322 (2011).
[14] Y. S. Cho, S. Hwang, H. J. Herrmann, and B. Kahng, Science **339**, 1185 (2013).
[15] R. M. D'Souza and J. Nagler, Nat. Phys. **11**, 531 (2015).
[16] D. Lee, Y. S. Cho, and B. Kahng, J. Stat. Mech. (2016) 124002.
[17] J. Alvarado, M. Sheinman, A. Sharma, F. C. MacKintosh, and G. H. Koenderink, Nat. Phys. **9**, 591 (2013).
[18] M. Sheinman, A. Sharma, J. Alvarado, G. H. Koenderink, and F. C. MacKintosh, Phys. Rev. Lett. **114**, 098104 (2015).
[19] S. V. Buldyrev, R. Parshan, G. Paul, H. E. Stanley, and S. Havlin, Nature (London) **464**, 1025 (2010).
[20] W. Cai, L. Chen, F. Ghanbarnejad, and P. Grassberger, Nat. Phys. **11**, 936 (2015).
[21] J. Chalupa, P. L. Leath, and G. R. Reich, J. Phys. C **12**, L31 (1979).
[22] S. N. Dorogovtsev, A. V. Goltsev, and J. F. F. Mendes, Phys. Rev. Lett. **96**, 040601 (2006).
[23] A. V. Goltsev, S. N. Dorogovtsev, and J. F. F. Mendes, Phys. Rev. E **73**, 056101 (2006).
[24] G. J. Baxter, S. N. Dorogovtsev, K. E. Lee, J. F. F. Mendes, and A. V. Goltsev, Phys. Rev. X **5**, 031017 (2015).
[25] D. Lee, M. Jo, and B. Kahng, Phys. Rev. E **94**, 062307 (2016).
[26] S.-W. Son, P. Grassberger, and M. Paczuski, Phys. Rev. Lett. **107**, 195702 (2011).
[27] D. Zhou, A. Bashan, R. Cohen, Y. Berezin, N. Shnerb, and S. Havlin, Phys. Rev. E **90**, 012803 (2014).
[28] S. Boccaletti, G. Bianconi, R. Criado, C. I. Del Genio, J. Gómez-Gardeñes, M. Romance, I. Sendina-Nadal, Z. Wang, and M. Zanin, Phys. Rep. **544**, 1 (2014).
[29] D. Lee, S. Choi, M. Stippinger, J. Kertesz, and B. Kahng, Phys. Rev. E **93**, 042109 (2016).
[30] Y. S. Cho, J. S. Lee, H. J. Herrmann, and B. Kahng, Phys. Rev. Lett. **116**, 025701 (2016).
[31] K. Panagiotou, R. Sphöel, A. Steger, and H. Thomas, Elec. Notes Discret. Math. **38**, 699 (2011).
[32] E. Ben-Naim and P. L. Krapivsky, Phys. Rev. E **71**, 026129 (2005).
[33] R. A. da Costa, S. N. Dorogovtsev, A. V. Goltsev, and J. F. F. Mendes, Phys. Rev. E **89**, 042148 (2014).
[34] R. A. da Costa, S. N. Dorogovtsev, A. V. Goltsev, and J. F. F. Mendes, Phys. Rev. E **90**, 022145 (2014).
[35] S. M. Oh, S.-W. Son, and B. Kahng, Phys. Rev. E **93**, 032316 (2016).
[36] M. E. Fisher, S.-K. Ma, and B. G. Nickel, Phys. Rev. Lett. **29**, 917 (1972).
[37] E. Fehr, J. S. Andrade, Jr., S. D. da Cunha, L. R. da Silva, H. J. Herrmann, D. Kadau, C. F. Moukarzel, and E. A. Oliveira, J. Stat. Mech. (2009) P09007.
[38] N. A. M. Araújo and H. J. Herrmann, Phys. Rev. Lett. **105**, 035701 (2010).
[39] M. E. Fisher and A. N. Berker, Phys. Rev. B **26**, 2507 (1982).